THE JOURNAL OF PHYSICAL CHEMISTRY B

ARTICLE

pubs.acs.org/JPCB

Cy3 in AOT Reverse Micelles II. Probing Intermicellar Interactions Using Fluorescence Correlation Spectroscopy

Jeffrey T. McPhee, Eric Scott, Nancy E. Levinger,* and Alan Van Orden*

Colorado State University, Department of Chemistry, Fort Collins, Colorado 80523, United States

ABSTRACT: Cyanine-3 (Cy3) fluorescent dye molecules confined in sodium di-2-ethylhexyl sulfosuccinate (AOT) reverse micelles were examined using dynamic light scattering and fluorescence correlation spectroscopy to probe the kinetics of Cy3 dye and reverse micelle aggregation. This study explored a range of reverse micelle sizes, defined as $w_0 = [H_2O]/[AOT]$, in which the occupation number ranged from one Cy3 molecule per $\sim 10^5$ to $\sim 10^6$ reverse micelles. These measurements reveal that in the smallest reverse micelle, $w_0 = 1$, the Cy3 molecules aggregate to form H-aggregate dimers, and the Cy3 dimerization is accompanied by the formation of a transient dimer between reverse micelles. Transient reverse micelle dimer particles are only observed in the small fraction of Cy3-labeled reverse micelles probed by fluorescence correlation spectroscopy and are not observed in the bulk solution probed by dynamic light scattering. Furthermore, fluorescence correlation spectroscopy makes it possible to probe the size and shape of these dimers, revealing prolate ellipsoid-shaped particles with twice the volume and surface area of a single reverse micelle.

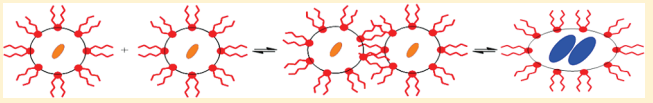

INTRODUCTION

The properties of sodium di-2-ethylhexyl sulfosuccinate (AOT) reverse micelles have a rich history of investigation[1] partially due to their utility to probe the effects of confinement on various molecular processes such as catalysis,[2−5] intermolecular charge transfer,[6] and redox reactions.[7,8] AOT reverse micelles form when the appropriate amounts of water, surfactant, and a nonpolar solvent are added together and consist of a water pool, surrounded by an interfacial region defined by the polar headgroups of the surfactant and aliphatic tails that penetrate into the nonpolar solvent.[9−21] The size of reverse micelles can be controlled by varying the concentration of water and surfactant in the system and is defined as w_0, governed by the equation[22]

$$w_0 = \frac{[H_2O]}{[\text{surfactant}]} \quad (1)$$

where [AOT] and $[H_2O]$ are the molar concentrations of each species in the nonpolar solvent. The hydrodynamic radius of AOT reverse micelles is on the order of nanometers given by[22]

$$R_H\ (\text{nm}) = 0.175w_0 + 1.5 \quad (2)$$

where R_H is the hydrodynamic radius. Studies have shown that the dynamic AOT reverse micelle system consists on average of spherical particles.[1] These spherical particles have been characterized using a range of techniques, including dynamic light scattering (DLS), which has determined both size and diffusion properties for AOT reverse micelles.[23] DLS measurements probe the ensemble average of reverse micelles in a bulk solution and are not sensitive to dynamic processes that may influence the molecular level interactions between the reverse micelles.

Only a few studies report the kinetics of intermicellar interactions. Fletcher et al. investigated exchange reactions involving proton transfer, electron transfer, and metal−ligand complexation.[22] Their investigation suggested the existence of a transient dimer that forms between the reverse micelles. This structure depends on the diffusion-limited collision between two reverse micelles. Subsequently, an encounter pair is formed in which the two reverse micelles are in contact, followed by coalescence of the reverse micelles to form the transient dimer. Although Fletcher et al. predicted its existence, the limited time resolution precluded confirmation of the transient dimer. However, on the basis of indirect observation, they inferred a lifetime of the transient dimer on the order of 25 μs.[22]

Fluorescence correlation spectroscopy (FCS) permits the study of dynamic processes occurring on time scales that range from nanoseconds to milliseconds.[24−30] Therefore, by labeling the reverse micelles with a fluorescent molecule, FCS can reveal the nature of intermicellar interactions. Measuring fluorescence fluctuations that are brought about by diffusion and other dynamic processes allows information about the kinetics of the system to be determined.

In an accompanying manuscript, we reported the observation of Cy3 H-aggregates in AOT reverse micelles.[31] This unique behavior of the dye has provided the opportunity to probe intermicellar interactions that we report here. Our FCS measurements suggest that the formation of the Cy3 H-aggregate also induces the formation of a transient reverse micelle dimer. The formation of the transient dimer causes the diffusion properties within the reverse micelle system to change, leading to a small subset of Cy3-labeled reverse micelles that diffuse more slowly than the rest. Here we present results from FCS and DLS

Received: January 5, 2011
Revised: June 15, 2011
Published: July 18, 2011

ACS Publications © 2011 American Chemical Society

measurements as well as a kinetic analysis describing the dimerization of the Cy3 dye and the reverse micelles.

EXPERIMENTAL METHODS

Sample Preparation. Cy3 monoreactive dye pack (GE Life Science) and *iso*-octane (99.8%, Sigma-Aldrich) were used as received. AOT (sodium di-2-ethylhexyl sulfosuccinate, 99%, Sigma-Aldrich) was purified using a process described elsewhere.[32] For sample preparation, the solid dye was dissolved in deionized Millipore water (18.2 MΩ cm), and the resulting solution was stored under refrigeration. Aqueous Cy3 solutions were prepared with a concentration range from 9.9×10^{-5} to 9.9×10^{-6} M. Cy3 showed no solubility in the pure *iso*-octane nonpolar phase in the absence of AOT.

Reverse micelles were prepared by dissolving AOT in *iso*-octane to form a 0.3 M stock solution to which aqueous dye solution and water were added. All samples were prepared using 2 mL of a 0.3 M AOT in *iso*-octane and 10.8 μL of an aqueous Cy3 solution. The size (w_0) and concentration of the reverse micelles were then adjusted by adding an appropriate amount of *iso*-octane and water, totaling 1 mL, resulting in a reverse micelle sample with an overall AOT concentration of 0.2 M. For the experiments reported here, the AOT concentration in the final solution was 0.02 M, unless otherwise noted. To make these final samples, a 100 μL aliquot of a 0.2 M AOT sample was diluted in 900 μL of isooctane. The final dye concentration ranged from 3.6×10^{-8} to 8.9×10^{-10} M. Using data in the literature,[33] we estimate that in the most concentrated samples we have at most one Cy3 molecule per 20 000 reverse micelles; at the lowest dye concentration, there is fewer than one dye molecule per 900 000 reverse micelles.

Dynamic Light Scattering Measurements. DLS measurements were performed using a Dyna Pro Titan instrument (Wyatt Technology). Samples were measured in ten 10 s scans. The hydrodynamic radii of the reverse micelle samples were obtained from an autocorrelation analysis of the scattered light using the Dynamics software.

Fluorescence Correlation Spectroscopy Measurements. FCS was used to probe the dynamics of the Cy3-labeled reverse micelles. The experimental procedure and setup for the FCS experiments have been previously reported.[24,34,35] In brief, the sample was placed into a well-slide and covered with a microscope cover slide, which sealed to the well-slide to prevent evaporation. The well-slide was treated with Sigmacote (Sigma-Aldrich) to prevent the Cy3 molecules from sticking to the glass cover slide. Prior to FCS experiments, well-slides were stored overnight in Piranha solution to ensure cleanliness. Before use, the well-slides were rinsed with water and placed in an oven for 10 min and then cooled to room temperature. The sample was placed on the stage of a Nikon Eclipse TE-2000-U microscope (Nikon, Melville, NY) and irradiated with a CW laser beam at either 514 nm (Ar ion laser, Melles-Griot) or 532 nm (Nd/YAG laser, B & W Tek) using a 100× 1.3 numerical aperture microscope objective. The laser power was 0.05 mW, before entering the microscope. The resulting fluorescence and laser light were transmitted back through the microscope. Fluorescence was separated from the incident laser light with a dichroic mirror, which transmitted the fluorescent light at a 90° angle. Upon exiting the microscope, the fluorescence was split by a 50/50 beam splitter and imaged onto two 50 μm confocal pinholes. The resulting light was band-pass-filtered and focused onto two single-photon-counting avalanche photodiode detectors (PerkinElmer). The resulting output of the detectors was recorded using the two channels of an ALV-5000E/EPP card (ALV) interfaced to a computer. Samples underwent 10, 200 s scans. For data analysis, the scans were averaged and plotted in a graphical analysis program (Igor Pro version 5.03). The fitting routine was performed using this same data analysis program.

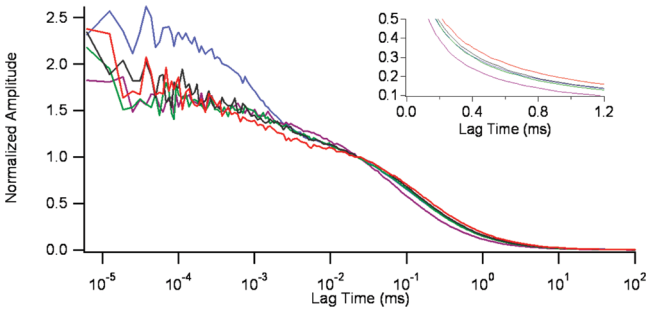

Figure 1. Autocorrelation functions of Cy3 from fluorescence correlation spectroscopy experiments in five different reverse micelle samples of varying size; w_0 = 1 (blue), 2 (purple), 9 (green), 15 (black), and 30 (red). The concentrations of Cy3 and AOT in all samples are 3.56×10^{-8} and 0.02 M, respectively. The inset highlights the region of the autocorrelation functions dominated by pure diffusion of the reverse micelles.

RESULTS

In the preceding paper, we reported the presence of H-dimers in the smallest reverse micelles, w_0 = 1, using a steady-state and time-resolved fluorescence techniques.[31] These results inform our understanding of the dynamics of this system, as studied using FCS.

FCS measures the fluorescence fluctuations of particles diffusing through an optical probe region created by focusing an excitation laser beam to a diffraction limited spot.[25,28,36] The fluctuations are analyzed to produce an autocorrelation function, which characterizes the time-dependent properties of the fluctuations occurring on time scales ranging from nanoseconds to milliseconds. On the longest time scale, the autocorrelation function reflects the particle diffusion time, τ_d, which represents the average diffusion time of single particles through the optical probe region. Measurement of τ_d characterizes the diffusion properties of the particle and is governed by the equation[25]

$$\tau_d = \frac{\omega_0^2}{4D} \tag{3}$$

where, ω_0 is the radius of the laser beam focus and D is the diffusion coefficient of the particle. Through calibration measurements, we determined $w_0 \approx 0.241 \pm 0.012$ μm in our experiment. The diffusion coefficient is determined by the equation[25]

$$D = \frac{k_B T}{6\pi\eta R_H} \tag{4}$$

where, k_B is the Boltzmann constant, T is the temperature, and η is the viscosity of the solution, assumed to be the same as the *iso*-octane solvent, 0.473 mPa·s.[37] R_H is the hydrodynamic radius of the diffusing particle. The experiments were carried out at the lab temperature of 21 °C. Because the Cy3 dye is completely insoluble in *iso*-octane, the observed fluorescence in our experiments arises from the Cy3 dye associated with the reverse

dx.doi.org/10.1021/jp2001282 |J. Phys. Chem. B 2011, 115, 9585–9592

Scheme 1. Structure of Cy3

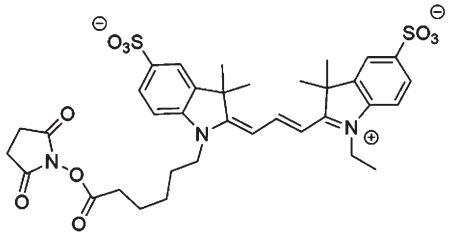

Table 1. Hydrodynamic Radii of Different Size Reverse Micelle Samples Determined Experimentally by Fluorescence Correlation Spectroscopy (FCS) and Dynamic Light Scattering (DLS) and Estimated Theoretically by Equation 2[a]

size (w_0)	FCS R_H (nm)	DLS R_H (nm)	theoretical R_H (nm)
30	5.4 ± 0.6	7.4 ± 0.4	6.8
15	4.2 ± 0.5	3.7 ± 0.1	4.1
9	3.9 ± 0.4	2.8 ± 0.1	3.1
2	2.5 ± 0.3	2.1 ± 0.1	1.9
1	2.2 ± 0.3,[b] 4.4 ± 0.3[c]	1.8 ± 0.3	1.7

[a] Concentration of Cy3 is 3.6×10^{-8} M and the concentration of AOT is 0.02 M. [b] Hydrodynamic radius for $w_0 = 1$ reverse micelles measured at 532 nm excitation. [c] Hydrodynamic radius for $w_0 = 1$ measured at 514 nm excitation.

micelles. Hence, the measured value of τ_d characterizes the diffusion of the reverse micelles, not of the free dye in solution.

Figure 1 shows the characteristic autocorrelation functions of Cy3 (Scheme 1) in five differently sized reverse micelles excited at 514 nm. The largest reverse micelle system displays an autocorrelation function with exponential decay on the submillisecond time scale consistent with translational diffusion of isolated reverse micelles. On the submicrosecond time scale, we observe a dynamic process that is consistent with previous FCS studies for Cy3 in aqueous solution.[29] As the reverse micelles become smaller, the autocorrelation function decays more rapidly, consistent with faster diffusion of the micelles. The dynamics occurring on shorter time scales exhibit similar behavior for micelles ranging from $w_0 = 30$ to 2. We analyzed the autocorrelation functions for $w_0 = 30$ to 2 shown in Figure 1 using the equations

$$g_D(\tau, \tau_d) = \left(\frac{1}{1 + \tau/\tau_d}\right)\left(\frac{1}{1 + \kappa_0^2\tau/\tau_d}\right)^{1/2} \quad (5)$$

$$G(\tau) - 1 = Ag_D(\tau, \tau_d)(1 + Be^{-\tau/\tau_{rxn1}}) \quad (6)$$

In eq 5, $g_D(\tau, \tau_d)$ is the pure diffusion autocorrelation function, τ_d is the average diffusion time through the optical probe volume, and κ_0 is the ratio (ω_0/z_0) of the radial, ω_0, and axial, z_0, confocal radii. The value of κ_0 was determined for our optical setup via control experiments to be ~0.10 and has been held fixed to this value in all fitting procedures. In eq 6, A is the amplitude of the autocorrelation function, B relates to the fraction of molecules undergoing dynamics on the shorter time scale, and τ_{rxn1} is the time constant for the process occurring on the shorter time scale. Using eq 3, we calculated the diffusion coefficient for each reverse micelle sample and determined the hydrodynamic radii using eq 4 (Table 1). We corroborated our FCS results using DLS, which is also shown in Table 1. The results for both techniques are consistent for $w_0 = 30$ to 2.

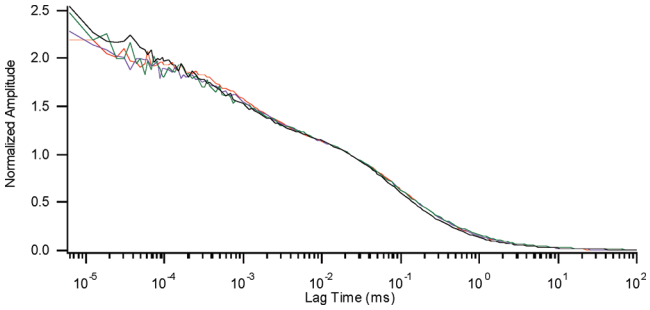

Figure 2. Autocorrelation curves of 1.8×10^{-9} M Cy3 in a 0.02 M AOT $w_0 = 1$ reverse micelle sample from fluorescence correlation spectroscopy experiments at four different laser excitation powers: 0.1 (red), 0.2 (blue), 0.9 (green), and 2.4 mW (black).

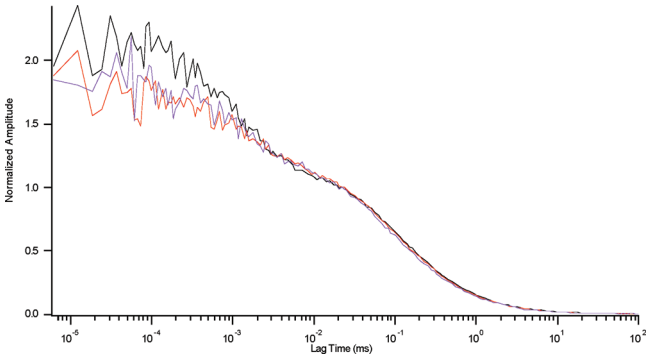

Figure 3. Two-color cross-correlation curves of 3.56×10^{-8} M Cy3 in a 0.02 M AOT $w_0 = 1$ reverse micelle sample. The fluorescence emission was detected by cross-correlating the detectors using different emission filters; detector 1 650 ± 15 nm band-pass−detector 2 600 ± 15 nm band-pass (black), detector 1 570 ± 15 nm band-pass−detector 2 600 ± 15 nm band-pass (red), and detector 1 570 ± 15 nm band-pass−detector 2 650 ± 15 nm band-pass (purple).

However, when the size of the reverse micelle is reduced to $w_0 = 1$, an abrupt change in the autocorrelation function occurs. First, we observe a dramatic increase in the amplitude of the autocorrelation function on the shorter time scales, which suggests that a new dynamic process occurs on the submicrosecond time scale in the $w_0 = 1$ reverse micelle samples. Various processes could be responsible for the reaction we observe occurring on the submicrosecond time scale for Cy3 in $w_0 = 1$ reverse micelles excited at 514 nm. These include intersystem crossing, aggregation, or isomerization.[27−30] We performed two additional experiments to explore whether these processes could account for the submicrosecond time scale signal. Both intersystem crossing, which leads to triplet blinking, and isomerization manifest as a dark state. With increasing laser power, both of these processes should increase the intensity of the submicrosecond feature.[27,29,30] Figure 2 shows the autocorrelation of FCS data collected with varying laser intensity. We observed no measurable change in the amplitude of the submicrosecond process with laser power. This suggests that confinement in the $w_0 = 1$ reverse micelle enhances neither triplet blinking nor isomerization and that these processes are not responsible for the

dx.doi.org/10.1021/jp2001282 |J. Phys. Chem. B 2011, 115, 9585–9592

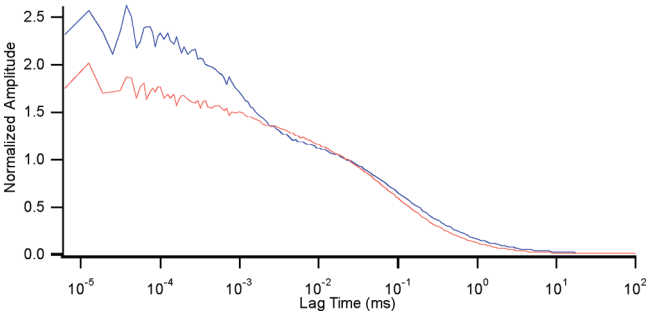

Figure 4. Autocorrelation curves of Cy3 in a w_0 = 1 reverse micelle sample from fluorescence correlation spectroscopy experiments at two different excitation wavelengths: 514 (blue) and 532 nm (red). The concentration of Cy3 is 3.56×10^{-8} M and the concentration of AOT is 0.02 M AOT.

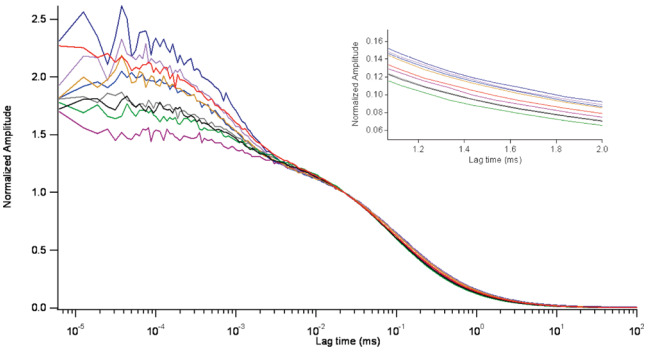

Figure 5. Autocorrelation curves of Cy3 in a w_0 = 1 reverse micelle sample from fluorescence correlation spectroscopy experiments at different overall Cy3 concentrations: 8.93×10^{-10} (dark purple), 1.78×10^{-9} (green), 3.56×10^{-9} (gray), 5.4×10^{-9} (black), 7.13×10^{-9} (red), 8.93×10^{-9} (light blue), 1.78×10^{-8} (gold), 2.67×10^{-8} (purple), and 3.56×10^{-8} M (dark blue). The concentration of AOT in all samples is 0.02 M. The inset highlights the region of the autocorrelation functions dominated by pure diffusion of the reverse micelles.

observed changes in the autocorrelation function. A previous study showing that trans−cis isomerization of the Cy3 monomer is likely suppressed in w_0 = 1 reverse micelles supports the interpretation that isomerization does not account for the submicrosecond feature.[31]

A second experiment investigated whether the association/dissociation of the Cy3 aggregate caused the submicrosecond fluctuation. From our previous results,[31] we know that emission at different wavelengths corresponds to monomer or aggregate forms of Cy3. If aggregation was occurring, then emission associated with the monomer form of the dye observed at 570 nm should correlate with emission at 600 or 650 nm as the aggregate dissociates to form the monomer and monomers join to form aggregates. Using filters on the two separate detectors, we monitored three separate two-color fluorescence cross-correlation functions: 570 nm with 600 nm; 570 nm with 650 nm; and 600 nm with 650 nm. Results shown in Figure 3 reveal that the cross-correlation amplitude of this process does not depend significantly on the combination of the 570 nm wavelength with the two other wavelengths. This suggests the submicrosecond fluctuations do not arise from association or dissociation of the Cy3 H-dimer. However, we do see a slight increase in the amplitude when cross-correlating the fluorescence at 600 and 650 nm. Our previous work showed that emission at 600 and 650 nm is due to the Cy3 aggregate.[31] Therefore, we hypothesize that the submicrosecond dynamic process is related to the dynamics of the dimer form of the dye that occurs in the w_0 = 1 reverse micelle.

In addition to the abrupt increase in the autocorrelation amplitude for the fast time scale process, the autocorrelation function of the w_0 = 1 sample also shows longer diffusion time compared with the larger reverse micelles. A comparison of the autocorrelation functions for w_0 = 1 and 2 samples shown in Figure 1 reveals that the w_0 = 1 reverse micelles diffuse more slowly than the w_0 = 2 reverse micelles, which contradicts the expected trend observed for the larger reverse micelles. By contrast, DLS measurement of identically prepared samples of Cy3-labeled w_0 = 1 reverse micelles diffuses faster than the w_0 = 2 reverse micelles. The apparent discrepancy between the DLS and FCS results can be explained by considering that the FCS experiment probes only a minute fraction of reverse micelles in solution, those containing the Cy3 dye, whereas DLS probes the entire ensemble. Thus, FCS experiments reveal slower diffusion for Cy3-containing reverse micelles than the overall ensemble of reverse micelles, whereas DLS analysis shows that the reverse micelles that contain no Cy3 dye molecules diffuse as expected, leading to a measured diffusion constant and hydrodynamic radius that agree with literature values.[23]

To investigate further the dynamics of Cy3 in the w_0 = 1 reverse micelles and the slower diffusion behavior, we measured autocorrelation functions at two different excitation wavelengths, 514 and 532 nm (Figure 4). Our previous work demonstrated that 514 nm radiation primarily excites the Cy3 dimer, whereas 532 nm primarily excites the monomer form of the dye in w_0 = 1.[31] Furthermore, from our previous work, we observe an equilibrium distribution of Cy3 monomers and Cy3 dimers in the w_0 = 1 reverse micelle samples, which can be characterized by selective excitation at the different wavelengths. Interestingly, the autocorrelation function for Cy3 in w_0 = 1 reverse micelles excited at 532 nm appears similar to the autocorrelation function for Cy3 in larger reverse micelles, particularly with respect to the process occurring on shorter time scales. Using the FCS data and eqs 3−6, we determined the hydrodynamic radius for the w_0 = 1 reverse micelles excited at 532 nm. The results of our analysis reveal reverse micelles with sizes commensurate with the DLS measurement for w_0 = 1, as shown in Table 1. Therefore, we do not observe the slower diffusion behavior when exciting at 532 nm. Because 532 nm radiation selectively excites the subpopulation of Cy3 monomers, whereas 514 nm selectively excites Cy3 dimers, these results indicate that Cy3 monomers are associated with isolated reverse micelles, whereas Cy3 dimers are associated with reverse micelle dimers.

If dimerization accounts for the slower diffusion observed, then the diffusion behavior should depend on the Cy3 concentration. Our previous study showed that increasing the Cy3 concentration shifted the equilibrium toward dimer formation.[31] Hence, if slower diffusion is related to dimer formation, this effect should become more pronounced as the Cy3 concentration increases. Autocorrelation functions from FCS measurements on samples containing varying concentrations of Cy3 dye while holding the concentration of reverse micelles constant and exciting at 514 nm to excite selectively the Cy3 aggregates appear in Figure 5. The autocorrelation function for the lowest concentration of Cy3 is qualitatively similar to our results for larger

size reverse micelles as well as results for Cy3 in $w_0 = 1$ excited at 532 nm. However, as the concentration increases, the amplitude of the short time scale process and the width of the autocorrelation function both increase. Despite the exceedingly low overall Cy3 concentrations probed, the increased amplitude of the short time process and the increased width of the autocorrelation function supports the hypothesis that Cy3 dimerization leads to the features of slower diffusion observed in the FCS results.

DISCUSSION

The results and analysis of our DLS and FCS experiments performed on the reverse micelles ranging in size from $w_0 = 30$ to 2 are consistent with our expectation that the Cy3 exists primarily as monomer and that the reverse micelles diffuse as independent particles. This behavior is also observed for the $w_0 = 1$ reverse micelles when exciting the sample at 532 nm, which is consistent with our previous work in which we deduced that 532 nm light primarily excites the monomer form of Cy3 inside the $w_0 = 1$ reverse micelles.[31]

However, when Cy3 in $w_0 = 1$ reverse micelles are analyzed with 514 nm excitation, we observe slower diffusion than for independent, isolated $w_0 = 1$ reverse micelles, as observed by DLS and FCS with 532 nm excitation. The FCS experiments probe only reverse micelles labeled with Cy3 dye molecules, whereas the DLS experiments probe the entire reverse micelle ensemble in the sample. The fraction of reverse micelles labeled with dye is ~45 ppm. Therefore, this slower diffusion is observed only in the minuscule fraction of dye-labeled reverse micelles and only when excited at 514 nm. Furthermore, the DLS measurements suggest that the bulk of the reverse micelles, which are not labeled with Cy3, diffuse with characteristics of regular AOT reverse micelles.[1] We suggest that the slower diffusion observed in the $w_0 = 1$ reverse micelles excited at 514 nm is related to Cy3 dimerization in a minuscule fraction of the reverse micelles

The observation that slower diffusion occurs only with 514 nm excitation and not at 532 nm excitation further suggests there are two subpopulations of dye-labeled reverse micelles when $w_0 = 1$, those that contain Cy3 dimers with longer diffusion times and those that contain Cy3 monomers and have a shorter diffusion time. The diffusion times observed for Cy3 in reverse micelles excited at 532 nm is consistent with independently diffusing micelles. However, the slower diffusion observed in reverse micelles excited at 514 nm suggests that not only are the Cy3 molecules dimerized but also dimerization of the reverse micelles accompanies dimerization of Cy3. These dimers of $w_0 = 1$ reverse micelles are thus responsible for the prolonged diffusion times.

In our previous work, we saw significant changes in the fluorescence emission spectra of Cy3 in $w_0 = 1$ reverse micelles as the concentration of Cy3 increased, indicating an increase in the amount of dimerization.[31] The changes in the autocorrelation function of Cy3 in $w_0 = 1$ reverse micelles as the concentration of Cy3 increases suggests that these changes are associated with the aggregate form of the Cy3 dye. At the lowest concentration, the autocorrelation function is qualitatively similar to those measured for the larger reverse micelles and the $w_0 = 1$ excited at 532 nm (Figures 1−3). This suggests that the Cy3 exists as a monomer at the lowest concentration. However, at the higher concentrations, the increased amplitude on the shorter time scale process and the increased width of the autocorrelation function

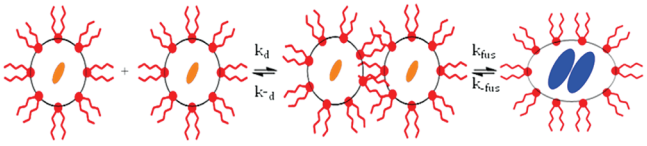

Figure 6. Proposed mechanism for the exchange reaction between two reverse micelles.

suggest that a different form of the dye is being probed and that this form of the dye is diffusing more slowly. To verify these results, we performed DLS measurements on samples of varying Cy3 concentration. Given the low Cy3 concentration leading to very low occupation numbers, fewer than one in 20 000, it is not surprising that the DLS experiments revealed no change in the bulk diffusion properties as a function of Cy3 concentration. This confirms that the changes observed in the FCS autocorrelation function are due to the small fraction of reverse micelles that have Cy3 molecules associated with them.

The spectroscopy and dynamics in the data presented thus far and in our previous work[31] show that in the $w_0 = 1$ reverse micelle the presence of Cy3 induces the dimerization of the dye and the reverse micelles. A mechanism consistent with our observations was proposed by the kinetic study previously described by Fletcher et al.[22] This study suggests the formation of a transient dimer with a ~25 μs lifetime. Hence, we propose that when Cy3 molecules in $w_0 = 1$ reverse micelles aggregate to form dimers, this dimerization is accompanied by the formation of a transient dimer between two Cy3-labeled reverse micelles.

Figure 6 shows a proposed mechanism for aggregation of Cy3 in $w_0 = 1$ reverse micelles, where individual Cy3 molecules are encapsulated by the individual reverse micelles. Upon colliding, the reverse micelles fuse together to create a transient dimer structure. This mechanism explains the spectroscopic changes as well as the longer diffusion time measured by FCS. It also explains why only a small fraction of the reverse micelles exhibit this behavior. Because the dye is present at such low concentrations, these transient dimers do not affect the entire bulk sample and are observed only in situations probing a select population of dye molecules.

To characterize further this mechanism, we have generalized the autocorrelation analysis in eq 3 to include contributions from both monomers and dimers as well as additional dynamic components using the following equation

$$G(\tau) = Ag_D(\tau, \tau_{d1}) + Bg_D(\tau, \tau_{d2})(1 + Ce^{-\tau/\tau_{rxn1}})(1 + Ee^{-\tau/\tau_{rxn2}}) \quad (7)$$

Here g_D is the pure diffusion autocorrelation function (eq 5), A is the fraction of molecules in the monomer form, τ_{d_1} is the diffusion time of the monomer, B is the fraction of molecules existing as dimers, and τ_{d_2} is the diffusion time of the transient reverse micelle dimer. In addition, eq 7 includes τ_{rxn1}, a fast decay in the autocorrelation function, and τ_{rxn2}, an intermediate decay. Moreover, the constants C and E relate to the fraction of molecules undergoing dynamics characterized by τ_{rxn1} and τ_{rxn2}, respectively. When fitting our data to this equation, we fixed the value of τ_{d_1} to that of individual $w_0 = 1$ reverse micelles determined by DLS. The value of τ_{d_2} was determined using the sample with the highest concentration of Cy3 in $w_0 = 1$ (Figure 3), which has minimal contribution from τ_{d_1} ($A \approx 0$).

dx.doi.org/10.1021/jp2001282 |J. Phys. Chem. B 2011, 115, 9585–9592

Table 2. Results of Fitting the Cy3 Concentration-Dependent Autocorrelation Functions to Equation 7[a]

overall Cy3 concentration (nM)	A	τ_{d1} (μs) fixed	B	τ_{d2} (μs) fixed	C	τ_{rxn1} (μs)	D	τ_{rxn2} (μs)
1.78	0.34 ± 0.02	70	0.33 ± 0.02	145	0.45 ± 0.02	0.9 ± 0.04	0.26 ± 0.01	11 ± 2
3.56	0.14 ± 0.02	70	0.25 ± 0.01	145	0.51 ± 0.03	1.0 ± 0.03	0.24 ± 0.01	15 ± 3
5.4	0.13 ± 0.03	70	0.28 ± 0.02	145	0.48 ± 0.04	1.0 ± 0.03	0.23 ± 0.02	18 ± 4
7.13	0.02 ± 0.005	70	0.09 ± 0.004	145	0.62 ± 0.03	0.9 ± 0.03	0.3 ± 0.01	10 ± 1
8.93	N/A	N/A	0.11 ± 0.003	145	0.56 ± 0.01	0.9 ± 0.02	0.19 ± 0.01	13 ± 1
17.8	N/A	N/A	0.04 ± 0.001	145	0.56 ± 0.01	0.9 ± 0.02	0.19 ± 0.01	15 ± 2
26.7	N/A	N/A	0.03 ± 0.001	145	0.66 ± 0.02	0.9 ± 0.03	0.19 ± 0.02	11 ± 2
35.6	N/A	N/A	0.015 ± 0.001	145	0.77 ± 0.04	1.0 ± 0.04	0.21 ± 0.03	9 ± 2

[a] Concentration of AOT is 0.02 M in all samples.

The results of fitting the concentration-dependent autocorrelation functions to eq 7 are shown in Table 2.

The FCS measurements described above can provide insight into the size and shape of the isolated reverse micelles and reverse micelle dimers. Using eq 3 and the value of τ_{d1} from Table 2, we obtain $D \approx 2.1 \times 10^{-6}$ cm^2/s for the isolated $w_0 = 1$ reverse micelles. Assuming a spherical shape, this implies a hydrodynamic radius of ~2.2 nm for a single isolated reverse micelle based on the Stokes−Einstein equation (eq 4), in reasonable agreement with the theoretical value of ~1.7 nm for a $w_0 = 1$ reverse micelle. Likewise, using the value of τ_{d2} in Table 2, we obtain $D \approx 1.0 \times 10^{-6}$ cm^2/s for the reverse micelle dimer. We assume that the surface-to-volume ratio of the merged particles will preclude the new particles from taking on a spherical shape. Therefore, the dimers are assumed to take the shape of a prolate ellipsoid with twice the volume and surface area of a single reverse micelle. These conditions are satisfied by a prolate ellipsoid with major axis a = 3.6 nm and minor axis b = 2.6 nm. Using the formula for the diffusion constant of a prolate ellipsoid with random orientation[38]

$$D = \frac{kT \ln(2a/b)}{6\pi\eta a} \tag{8}$$

we obtain $D \approx 1.3 \times 10^{-6}$ cm^2/s. Conversely, if we assume a spherical-shaped reverse micelle dimer with twice the volume and surface area of a single reverse micelle, we obtain $D \approx 1.6 \times 10^{-6}$ cm^2/s. Hence, the prolate ellipsoid shape gives diffusion properties that are consistent with the observed behavior of the dimer particles, suggesting that the FCS measurements can successfully probe the structural properties of these particles.

We note that the fast time component of the autocorrelation functions in Figure 5 requires two exponential decays, τ_{rxn1} and τ_{rxn2}, to obtain a good fit. The time scale of τ_{rxn1} is independent of Cy3 concentration. However, the amplitude of this component increases with increasing concentration, suggesting that the reaction being probed on this time scale represents the interplay between monomer and dimer. In our analysis above, we eliminated the possibility that triplet blinking or the association/dissociation of the Cy3 aggregate causes this process. Likewise, because the rotational correlation time for the transient dimer should be ~15 ns, which is much faster than the fluctuation observed on this 1 μs time scale, we rule out rotational correlation of the transient dimer as the source of this fluctuation. Although the exact process responsible for this fluctuation remains unclear, we believe it reflects a conformational fluctuation of the Cy3 dimer that causes an intensity fluctuation in the autocorrelation function, consistent with our cross-correlation analysis of 600 and 650 nm, previously described.

The second time constant, τ_{rxn2}, was measured to be on the order of 10 to 20 μs. This time constant was also independent of Cy3 concentration. On the basis of indirect analysis, Fletcher et al.[22] deduced that the transient micelle dimer has a lifetime on the order of tens of microseconds. We hypothesize that τ_{rxn2} could be due to a dynamic process within the Cy3 H-dimer that is coupled to the lifetime of the reverse micelle dimer, although the exact nature of this coupling is not clear. If this process is not related to the formation of the transient reverse micelle dimer, then the dimer is most likely stable on a time scale longer than we can measure using FCS and longer than Fletcher et al. predicted.

The data presented here and in our previous work[31] suggest that both the Cy3 dye and the reverse micelles interact to form dimers. We propose a mechanism shown in Figure 6. Here two reverse micelles, each containing a Cy3 monomeric dye molecule, collide. Following this collision, the reverse micelles conjoin, promoting the interaction and dimerization of the Cy3 molecules. The overall equilibrium for the process shown in Figure 6 is given by

$$K_{overall} = K_d K_{fus} = \frac{k_d}{k_{-d}} \frac{k_{fus}}{k_{-fus}} \tag{9}$$

where k_d and k_{-d} are the forward and reverse rate constants for reverse micelle encounter and k_{fus} and k_{-fus} are the forward and reverse rate constants for reverse micelle fusion and Cy3 dimerization. The data presented here were insufficient to determine each rate constant and equilibrium constant with confidence, specifically, assumptions required to determine rates of micelle fusion. However, we can estimate rates and equilibrium constants for the first step of the mechanism. We are pursuing additional experiments to determine rates directly from the data.

The initial step of the mechanism depicted in Figure 6 involves the collision of two Cy3-labeled reverse micelles. Translational diffusion of the reverse micelles limits the maximum forward rate for this process and can be described by[22]

$$k_d = \frac{8k_B T}{3\eta} \tag{10}$$

where k_B is the Boltzmann constant, T is temperature, and η is the viscosity of iso-octane. The conditions used yield $k_d = 1.4 \times 10^{10}$ L mol^{-1} s^{-1}. On the basis of this value, the Cy3 concentration, temperature, and viscosity values reported above, we predict an upper limit for the collision rate of two Cy3-labeled reverse micelles to be 5.0×10^2 s^{-1} (approximately one collision every

dx.doi.org/10.1021/jp2001282 |J. Phys. Chem. B 2011, 115, 9585–9592

2 ms). Although this rate is too slow to be measured by our FCS experiment, it provides a value that we can use to explore the rest of the steps in the mechanism.

To determine K_d, we require the rate constant for the separation of the encounter pair back to isolated reverse micelles, k_{-d}, which is defined by the equation[22]

$$k_{-d} = \frac{6D}{(2r)^2} \quad (11)$$

where, r is the radius of an individual reverse micelle. Using 2.1×10^{-10} m^2 s^{-1} for D, obtained from the FCS data using eq 4, and $r \approx 1.8 \times 10^{-9}$ m, the measured value of R_H from DLS for $w_0 = 1$ reverse micelles (Table 2), we calculated k_{-d} to be $\sim 1.1 \times 10^8$ s^{-1}, which yields $K_d = 124$ M^{-1}, and $\Delta G < 0$.

The data presented demonstrate that the smallest reverse micelles, $w_0 = 1$, form transient dimers that are stable on the time scale of our FCS experiment. We hypothesize that the reverse micelles undergo interactions that allow their contents to be exchanged. During this process, the reverse micelles form the transient dimer accompanied by the formation of a Cy3 dimer, which we observe in our FCS measurements and other spectroscopic studies.[31] We do not observe evidence of dimer formation in reverse micelles larger than $w_0 = 2$. This could reflect the less confined environment found in larger reverse micelles.

CONCLUSIONS

We report the direct observation of a transient reverse micelle dimer. The use of two different excitation wavelengths, 514 and 532 nm, allows us to probe the dynamics of both the Cy3 monomer-labeled reverse micelles and those reverse micelles containing the Cy3 H-dimer, consistent with our previous work. Moreover, the reverse micelles containing the Cy3 H-dimer exhibit slower diffusion behavior that is not seen in the isolated reverse micelles and in our DLS experiments. Furthermore, we have characterized the structural properties of the slower diffusing particles and found them to be consistent with a transient reverse micelle dimer having a prolate ellipsoid shape with twice the volume and surface area of a single reverse micelle. The results show that reverse micelles are dynamic, undergoing collisions and exchanging contents. Although these systems can be made up of discrete individual droplets, aggregates and bicontinuous structures like the transient dimer observed here can exist, thus altering the diffusion properties of the system. The results presented here suggest that reverse micelles can be used as a nanocatalyst to cause reactions to occur that would otherwise not occur, as seen by the formation of the Cy3 H-dimer at concentrations so dilute as to preclude aggregation in bulk aqueous solution.

AUTHOR INFORMATION

Corresponding Author

*E-mail: vanorden@lamar.colostate.edu (A.V.O.), levinger@lamar.colostate.edu (N.E.L.).

ACKNOWLEDGMENT

Funding for this work was provided by the National Science Foundation Collaborative Research in Chemistry grant number 0628260. We thank Debbie Crans and her research group for helpful discussions and assistance with sample preparation.

REFERENCES

(1) De, T. K.; Maitra, A. *Adv. Colloid Interface Sci.* **1995**, *59*, 95–193.
(2) Abuin, E.; Lissi, E.; Solar, C. *J. Colloid Interface Sci.* **2005**, *283*, 87–93.
(3) Correa, N. M.; Durantini, E. N.; Silber, J. J. *J. Org. Chem.* **1999**, *64*, 5757–5763.
(4) Martinek, K.; Levashov, A. V.; Klyachko, N.; Khmelnitski, Y. L.; Berezin, I. V. *Eur. J. Biochem.* **1986**, *155*, 453–468.
(5) Menger, F. M.; Yamada, K. *J. Am. Chem. Soc.* **1979**, *101*, 6731–6734.
(6) Novaira, M.; Moyano, F.; Biasutti, M. A.; Silber, J. J.; Correa, N. M. *Langmuir* **2008**, *24*, 4637–4646.
(7) Correa, N. M.; Zorzan, D. H.; Chiarini, M.; Cerichelli, G. *J. Org. Chem.* **2004**, *69*, 8224–8230.
(8) Correa, N. M.; Zorzan, D. H.; D'Anteo, L.; Lasta, E.; Chiarini, M.; Cerichelli, G. *J. Org. Chem.* **2004**, *69*, 8231–8238.
(9) Baruah, B.; Crans, D. C.; Levinger, N. E. *Langmuir* **2007**, *23*, 6510–6518.
(10) Baruah, B.; Roden, J. M.; Sedgwick, M.; Correa, N. M.; Crans, D. C.; Levinger, N. E. *J. Am. Chem. Soc.* **2006**, *128*, 12758–12765.
(11) Baruah, B.; Swafford, L. A.; Crans, D. C.; Levinger, N. E. *J. Phys. Chem. B* **2008**, *112*, 10158–10164.
(12) Correa, N. M.; Levinger, N. E. *J. Phys. Chem. B* **2006**, *110*, 13050–13061.
(13) Crans, D. C.; Baruah, B.; Levinger, N. E. *Biomed. Pharmacother.* **2006**, *60*, 174–181.
(14) Crans, D. C.; Rithner, C. D.; Baruah, B.; Gourley, B. L.; Levinger, N. E. *J. Am. Chem. Soc.* **2006**, *128*, 4437–4445.
(15) Crans, D. C.; Trujillo, A. M.; Bonetti, S.; Rithner, C. D.; Baruah, B.; Levinger, N. E. *J. Org. Chem.* **2008**, *73*, 9633–9640.
(16) Falcone, R. D.; Correa, N. M.; Biasutti, M. A.; Silber, J. J. *Langmuir* **2000**, *16*, 3070–3076.
(17) Harpham, M. R.; Ladanyi, B. M.; Levinger, N. E. *J. Phys. Chem. B* **2005**, *109*, 16891–16900.
(18) Harpham, M. R.; Levinger, N. E.; Ladanyi, B. M. *J. Phys. Chem. B* **2008**, *112*, 283–293.
(19) Moilanen, D. E.; Levinger, N. E.; Spry, D. B.; Fayer, M. D. *J. Am. Chem. Soc.* **2007**, *129*, 14311–14318.
(20) Roess, D. A.; Smith, S. M. L.; Winter, P.; Zhou, J.; Dou, P.; Baruah, B.; Trujillo, A. M.; Levinger, N. E.; Yang, X. D.; Barisas, B. G.; Crans, D. C. *Chem. Biodiversity* **2008**, *5*, 1558–1570.
(21) Tan, H. S.; Piletic, I. R.; Riter, R. E.; Levinger, N. E.; Fayer, M. D. *Phys. Rev. Lett.* **2005**, 94.
(22) Fletcher, P. D. I.; Howe, A. M.; Robinson, B. H. *J. Chem. Soc., Faraday Trans. I* **1987**, *83*, 985–1006.
(23) Zulauf, M.; Eicke, H. F. *J. Phys. Chem.* **1979**, *83*, 480–486.
(24) Fogarty, K.; McPhee, J. T.; Scott, E.; Van Orden, A. *Anal. Chem.* **2009**, *81*, 465–472.
(25) Van Orden, A.; Fogarty, K.; Jung, J. *Appl. Spectrosc.* **2004**, *58*, 122A–137A.
(26) Van Orden, A.; Jung, J. *Biopolymers* **2008**, *89*, 1–16.
(27) Widengren, J.; Mets, U.; Rigler, R. *J. Phys. Chem.* **1995**, *99*, 13368–13379.
(28) Widengren, J.; Rigler, R. *Cell. Mol. Biol.* **1998**, *44*, 857–879.
(29) Widengren, J.; Schwille, P. *J. Phys. Chem. A* **2000**, *104*, 6416–6428.
(30) Widengren, J.; Seidel, C. A. M. *Phys. Chem. Chem. Phys.* **2000**, *2*, 3435–3441.
(31) McPhee, J. T.; Scott, E.; Levinger, N. E.; Van Orden, A. *J. Phys. Chem. B* **2011**, in press. DOI: http://dx.doi.org/10.1021/jp200126f.
(32) Stahla, M. L.; Baruah, B.; James, D. M.; Johnson, M. D.; Levinger, N. E.; Crans, D. C. *Langmuir* **2008**, *24*, 6027–6035.
(33) Chowdhury, P. K.; Ashby, K. D.; Datta, A.; Petrich, J. W. *Photochem. Photobiol.* **2000**, *72*, 612–618.

(34) Jung, J.; Ihly, R.; Scott, E.; Yu, M.; Van Orden, A. *J. Phys. Chem. B* **2008**, *112*, 127–133.
(35) Jung, J. Y.; Van Orden, A. *J. Am. Chem. Soc.* **2006**, *128*, 1240–1249.
(36) Elson, E. L.; Magde, D. *Biopolymers* **1974**, *13*, 1–27.
(37) Padua, A. A. H.; Fareleira, J. M. N. A.; Calado, J. C. G. *J. Chem. Eng. Data* **1996**, *41*, 1488–1494.
(38) Dill, K. A.; Bromberg, S. *Molecular Driving Forces*; Garland Science: New York, 2011.